Analysis of Heat Transfer Performance of a Fork-End Heat Pipe using MARS-KS

Sangmin Park[a], Changhwan Lim[a], Jonghwi Choi[a], Hyungdae Kim[a*], Taewan Kim[b]
[a]*Nuclear Engineering, Kyung Hee University, Republic of Korea*
[b]*Safety and Environmental System Engineering, Incheon National University, Republic of Korea*
[*]*Corresponding author: hdkims@khu.ac.kr*

1. Introduction

It is clear that spent nuclear fuels continuously release residual heat due to radioactive decay of fission products. Since the Fukushima accident, importance of removal of such decay heat using passive cooling system against a station black-out accident of a nuclear power plant cannot be overemphasized. The passive cooling system has to prevent exposure of nuclear fuels over the coolant in order to ensure the safety criterion for surface temperature of cladding. Recently, several research groups were proposed passive system using heat pipes which are generally used passive heat exchanger in various field [1-3]. Lim and Kim [4] proposed a new concept of a large-scale fork-end heat pipe (FEHP) system for passive cooling of a spent fuel pool during a station blackout accident and experimentally examined heat transfer performance of a scale-downed FEHP.

In this study, heat transfer performance of the scale-downed FEHP was numerically analyzed using a best-estimate thermal-hydraulic analysis code, MARS-KS 1.4 [5]. The obtained results were compared with measurement data in [4].

2. Experiment

The schematic diagram of the FEHP and the experiment facility used in Lim and Kim [4] is shown in Fig. 1. Firstly, Fig.1(a) shows the FEHP. It consists of three main part: an evaporator, a header, a condenser. The evaporator is 1m long, 19.05mm outer diameter and 0.8mm thick. The condenser is 1m long, 12.7mm outer diameter and 0.8mm thick. The circular fins are attached to condenser tubes that are 9.65mm high and 0.5mm thick. The number of pins per condenser tube is 300. The 12-conductor tubes are connected to the manifold header (adiabatic zone). The header serves to collect condensed working fluid from the condenser tube. The condenser tube and header have an inclination of 7°. For this reason, condensate easily returns to the evaporator part. The working fluid is water. Secondly, Fig. 1(b) shows the experiment facility. It comprises two main parts: a heating loop and an air-cooling duct. The heating loop is filled with distilled water which is heated by immersion heaters in the chamber. In the heating loop, flow path is divided into the test section and the bypass. The flow rate of test section is controlled using a valve and a bypass. The heat pipe is installed in the center of circular water jacket of the test section thereby an annular flow passage is formed. The heat pipe is heated-up by hot water also cooled by upstream flow of air.

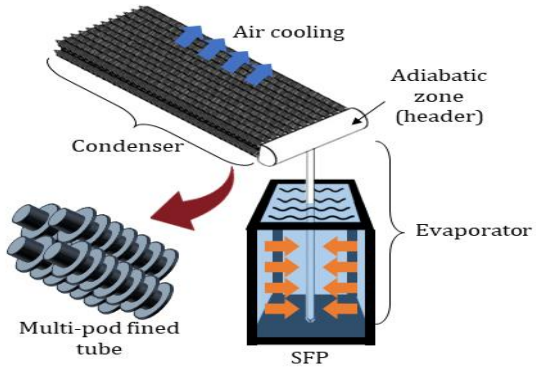

Fig. 1(a) Schematic of FEHP [4]

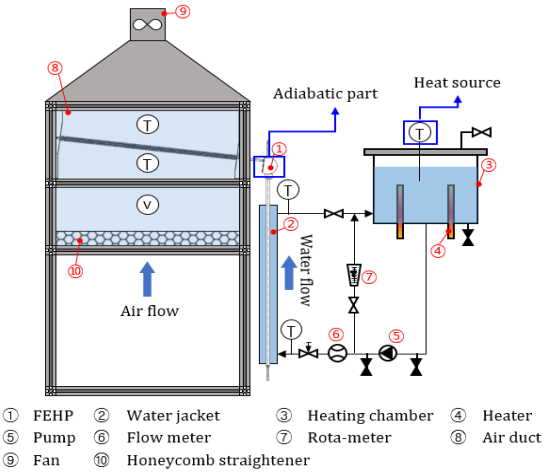

Fig. 1(b) Schematic of experiment facility [4]

In the air-cooling duct, a honeycomb-shaped mesh is installed at the bottom to form a uniform flow, and air flow is created using the upper fan. The experimentally measured heat transfer performance data are utilized to compare the results of MARS.

3. MARS Analysis

3.1 Nodalization

For numerical simulation of the above-described experiment, three major parts were modeled in MARS: a heating loop, a FEHP, and an air-cooling duct nodalization is shown in Fig. 2.

Firstly, the FEHP comprises evaporator, adiabatic part, condensers. Evaporator (component 130) consists of 12

nods with 0.1 m elevation per node, 10 nodes of which are connected to the left boundary of heat structure. 12th node of pipe is connected to single volume (component 120) that is adiabatic part. There are 12 condensers also each condenser has 11 nodes. All condensers are connected to the single volume (component 120) through the multiple junction (component 115). Those pipes are connected to left boundary of another heat structure. Finally, the right boundary of this heat structure is connected to time dependent volume (component 400) that is function as air-cooling duct.

The heating loop part consists of an inlet, a jacket and an outlet. The inlet and outlet part are made by time dependent volume (component 200 and 240) and single volume (component 210 and 230) that play a role for heating chamber and piping system, respectively. The jacket is made by pipe component (component 220) which has 10 nods with 0.1 m elevation per node. Above all volume components are connected with single junction except inlet junction (component 205). The inlet junction is made by time dependent junction that play a role for pump. It makes total flow rate through heating loop system. The nodes of Jacket (component 220) are connected with node of evaporator (component 130) through heat structure. The left and right boundary conditions of the heat structure are chosen as convective boundary condition.

3.2 Modeling of the air-cooling duct

Internal pressure of the heat pipe is determined by the boundary conditions at the heating loop and the air-cooling duct, such as convective heat transfer coefficient. There is no appropriate correlation for cross-flow convective heat transfer coefficient of finned tubes in the air-cooling duct. As the main focus of this analysis is not on air convection heat transfer coefficient of finned tubes but on the heat transfer characteristics of the heat pipe, the problem was modified to determine wall temperature of the finned tube which makes internal pressure of the heat pipe to be same as the measurement values obtained in the experiment. For this reason, the air-cooling duct was replaced by a time dependent volume and the outer wall of the condenser tubes was set to have a high heat transfer coefficient, which makes the outer wall temperature of the condenser tube to be same as the characteristic temperature of the time-dependent volume. Thus, temperature of the time-dependent volume determines directly affects internal pressure of the heat pipe.

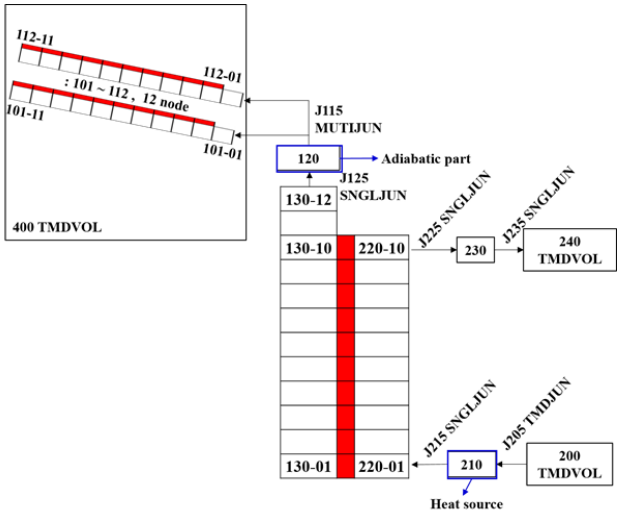

Fig. 2. Modeling of experimental device for FEHP heat transfer in MARS-KS

4. Results

4.1 Pressure

The internal pressure of the heat pipe determined in MARS is summarized in Table 1. The repetitive iteration with MARS code confirmed that the pressure of the heat pipe calculated by MARS was well converged with that of the experiment. As shown in Fig. 3, the heat pipe pressure of MARS analysis and experiment shows good matches in all heat source temperatures tested in the experiment.

Table 1. Pressure at the adiabatic part with heat source temperature in reduced scale experiment

Heat source temperature [K]	Measured pressure [Pa]
339.8	5500
340.8	5600
348.1	8600
354.9	12300
355.9	12200
356.0	12600
360.4	13300
365.2	15200
370.3	15600
371.5	15600

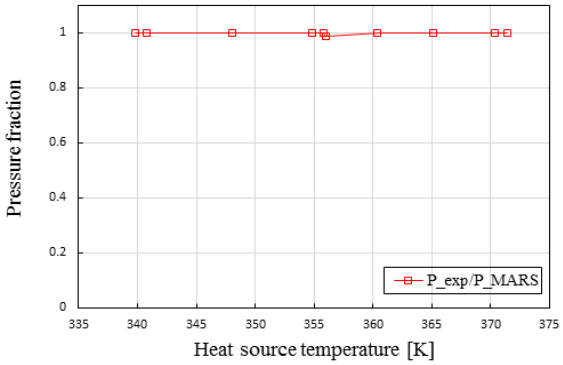

Fig. 3 Pressure ratio of experiment to MARS-KS code as a function of heat source temperature

4.2 Temperature

Fig. 4 shows a comparison of the temperature in adiabatic part measured in the experiment with those calculated by MARS code according to heat source temperature. The temperature of adiabatic part in MARS calculation does not exactly match the temperature of adiabatic part in the experiment, but it is similar in tendency and converges within the error range (±5K). Table 1 shows pressure at the adiabatic part with heat source temperature. The saturation temperature is the value calculated for the pressure measured in the experiment. Since MARS code calculates the working fluid as saturated, the temperature of the adiabatic part matches the saturation temperature. However, the current experiments have produced quantitative differences with the analysis results since temperature of the working fluid was measured in the adiabatic part as superheated vapor.

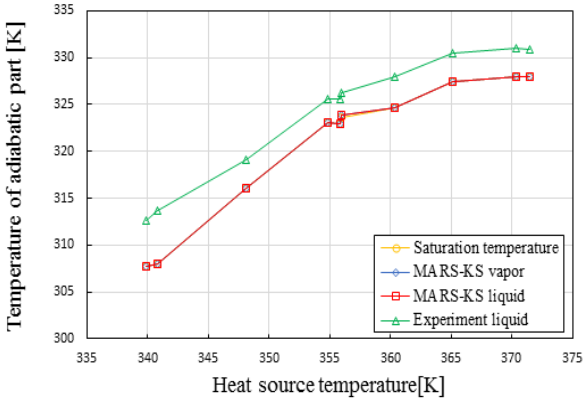

Fig. 4 Temperature at the adiabatic part of heat pipe as a function of heat source temperature

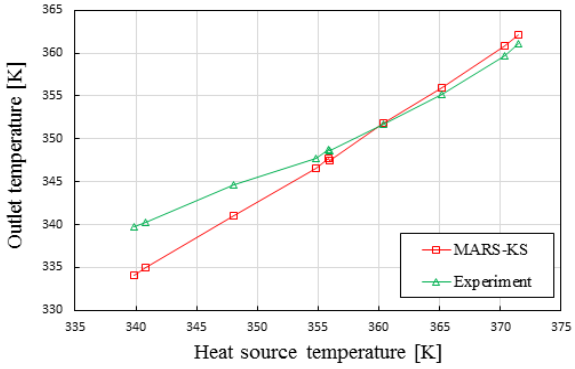

Fig. 5 Temperature of the heating fluid at the outlet as a function of heat source temperature

Fig. 5 shows a comparison of heat source outlet temperature measured in the experiment and calculated by MARS. At The heat source outlet temperature converges within the error range (±5K) when heat source temperatures are 339.8K, 340.8K, 348.1K. But those temperatures in the MARS calculation nearly match one in the experiment.

4.3 Heat transfer

Table 2 shows boiling regime in the evaporator of heat pipe according to the inlet fluid temperature in the heating loop (=heat source temperature). When the heat source temperature changes from 339.8K to 348.1K, the boiling regime is not fully developed, such as single-phase convection without boiling and intermittent boiling [6].

Table 2. Boiling regimes in the evaporator of the heat pipe observed in the experiment with respect to heat source temperature

Heat source temperature [K]	Boiling regime
339.8	No boiling
340.8	Intermittent boiling – geyser
348.1	
354.9	Fully developed boiling - nucleate pool boiling
355.9	
356.0	
360.4	
365.2	
370.3	Fully developed boiling - falling film boiling
371.5	

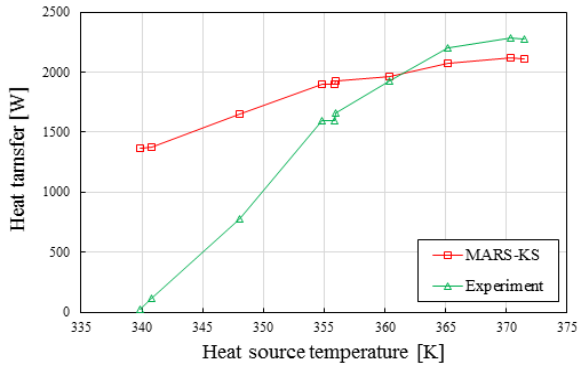

Fig. 6 Heat transfer in evaporator according to heat source temperature

Fig. 6 shows a comparison of the heat transfer in evaporator measured in the experiment with those obtained by MARS analysis according to heat source temperature. When the heat source temperature rises from 339.8K to 348.1K, there is a big difference of heat transfer between experiment and MARS result. From 354.9K, the results of the experiment and those calculated by MARS almost converges within the error range (20%). At heat source temperature less than 348.1K, boiling regime is not fully developed based on the above three results and the difference between experimental results and MARS results. In order to accurately simulate the heat transfer characteristics of FEHP, all the associated boiling regimes observed in the experiment should be properly modeled in MARS.

5. Conclusions

Heat transfer performance of a fork-end heat pipe designed and tested by Lim and Kim [4] was numerically analyzed using MARS-KS and compared to the experimental observation. The key findings from the present study are following:

- When characteristic system temperature of the heat pipe was higher than ~355K, the simulation results of heat transfer performance in comparison with the experimental measurement showed a reasonable agreement within error of 20%. Boiling heat transfer modes in the evaporator part of the heat pipe at relatively high load, including nucleate pool boiling and falling film boiling, seem to be properly modeled in MARS.
- When heat source temperature was lower than ~355K, considerable errors in the comparison of heat transfer and heating fluid temperature were observed. It was supposed that the boiling regime at such temperature could not be properly modelled in MARS, which results in a considerable discrepancy in heat transfer and system temperature between experiment and simulation.

Acknowledge

This work was supported by the Nuclear Power Core Technology Development Program of the Korea Institute of Energy Technology Evaluation and Planning (KETEP), and granted financial resources by the Ministry of Trade, Industry & Energy, Republic of Korea (No. 20151520101000)

REFERENCES

[1] Minglu Wang, Mingguang Zheng, Cheng Ye, Zhongming Qiu, and Zhenqin Xiong, An Experimental Study of Closed Loop Two-Phase Thermosyphon for Spent Fuel Pool Passive Cooling, Proceedings of the 2016 24th International Conference on Nuclear Engineering, June 26-30, Charlotte, North Carolina, 2016

[2] Kyung Mo Kim, In Cheol Bang, Heat transfer characteristics and operation limit of pressurized hybrid heat pipe for small modular reactors, Applied Thermal Engineering 112, 560–571, 2017

[3] Prevention Possibility of Nuclear Power Reactor Meltdown by Use of Heat Pipes for Passive Cooling of Spent Fuel, Masataka Mochizuki, Thang Nguyen, Koichi Mashiko, Yuji Saito, Randeep Singh, Tien Nguyen, and Vijit Wuttijumnong, Frontiers in Heat Pipes (FHP), 4, 013001, 2013

[4] Changhwan Lim, Hyungdae Kim, Experimental Study on Heat Transfer Characteristics of a Multi-Pod Heat Pipe, Transactions of the Korean Nuclear Society Autumn Meeting Gyeongju, October 26-27, Korea, 2017.

[5] KINS, MARS CODE MANUAL Vol.Ⅱ: Input requirements, 2018

[6] Guodong Xia, Wei Wanga, Lixin Cheng, Dandan Ma, Visualization study on the instabilities of phase-change heat transfer in a flat two-phase closed thermosiphon, Applied Thermal Engineering 116, 392-405, 2017